Interaction of Methane with a $[Li]^0$ Center on MgO(100): HF, Post-HF, and DFT Cluster Model Studies

L. Ackermann,[†] J. D. Gale,[‡] and C. R. A. Catlow*,[†]

Davy Faraday Research Laboratory, The Royal Institution, 21 Albemarle Street, London W1X 4BS, U.K., and Department of Chemistry, Imperial College, South Kensington, London SW7 2AY, U.K.

Received: July 7, 1997; In Final Form: August 26, 1997[⊗]

We investigate the interaction between methane and a $[Li]^0$ center on MgO(100) using ab initio cluster methodology. We focus on the catalytic activation of the C−H bond, an essential reaction step in the oxidative coupling of methane (OCM). In the first part of the study we use a simple embedded cluster model that allows us to compare different levels of theory and to study the influence of electron correlation on the calculated energy profile for the H abstraction reaction. Hartree−Fock (HF) calculations are compared to results obtained from post-HF (Møller−Plesset perturbation theory) and gradient-corrected density functional theory (DFT) computational schemes. We show that the use of the density functional exchange potential without self-interaction corrections leads to an inadequate potential energy surface for the hydrogen abstraction reaction at the $[Li]^0$ center. The second part of the study is devoted to substrate relaxation effects, employing a much larger cluster model. The geometry of the lattice around the $[Li]^0$ cener is optimized for key stages along the reaction path. Comparison with previous studies shows the importance of including extensive relaxation if accurate geometries about the surface defect sites are to be calculated.

1. Introduction

Formation of higher hydrocarbons from methane, $CH_4 \rightarrow C_2H_x$ is at the heart of several important industrial processes. It is no surprise, therefore, that the oxidative coupling of methane (OCM), representing one viable route to this end, has been examined in a variety of experimental and theoretical studies for many years now.[1,2] These investigations aim at characterizing the ideal conditions for catalyzed OCM and developing a detailed model of the catalytic process. Various oxides are known to be catalytically active, among them (doped or undoped) alkaline earth oxides, lanthanide oxides, transition metal oxides, as well as oxides of main group elements and complex oxides.[1]

Many improvements have been made to increase both the CH_4 conversion rate and the selectivity for desired products (i.e., C_2 hydrocarbons) as opposed to waste products (CO, CO_2). To do this in a systematic fashion, a detailed knowledge of the basic processes involved in catalytic OCM is necessary. Clearly, these involve the breaking of a CH bond and the formation of a CC bond. The latter is assumed to take place in the gas phase, whereas the former has been proposed to occur at the surface of the catalyst.[2] Little is known, however, about the CH bond-breaking step at a molecular level. A number of theoretical studies[3−13] have attempted to model this process, but the lack of experimental data makes it difficult to clarify the details of the mechanism involved.

Lithium-doped magnesium oxide, Li/MgO, may be called the prototypical catalyst system for OCM. It is relatively simple and has, therefore, been studied extensively. The centers that facilitate CH bond breaking are unlikely to be present on a perfect MgO surface. Candidates for the active site for this process include nonideal surface structures (like kinks, steps), cation and anion vacancies, substitutional ions (dopants), and surface hole states. It has been concluded from experimental evidence that electron holes localized on oxygen ions, forming O^- sites, are involved in the catalytic process.[14] This type of electronic defect is stabilized by a neighboring Li^+ ion (substituting for Mg^{2+}) to form a $[Li]^0$ center. Several theoretical investigations have used this type of defect as a model for the active site on Li/MgO.[4−8,15,12,13] Although the role of $[Li]^0$ centers in the process of CH bond breaking has recently been questioned,[2] it still seems to be the most probable model for the active site. Previous calculations confirming this proposal may suffer from the neglect of various aspects either in the computational methodology or in the model systems used (or in both). In this present study the catalytic effect of $[Li]^0$ centers on the initial reaction of an OCM process is investigated, paying special attention to the effects of the choice of computational techniques and to the models used to represent the active site.

In representing methane activation over a $[Li]^0$ center, one has to find a model capable of describing (i) the surface site and (ii) the reaction taking place. Adoption of the cluster approach to achieve (i) requires a careful choice of the model, since the Madelung field of the ions that are not included in the cluster exhibits a long-range effect. If it is neglected completely (as, for example, in ref 5), a model quite different from the actual surface site may result.

A simple and effective—though still somewhat crude—way to take into account the electrostatic contribution of the remaining solid (i.e., of the ions not explicitly included in the cluster) is used in many studies:[8,16−19] an array of point charges (PC) at bulk lattice positions is introduced to embed the cluster. Considering the nature of the defect, however, both polarization and relaxation of the substrate are known to occur. Neither of these effects can be represented by simple PC embedding, but more sophisticated schemes have been developed to take them into account.[20−22]

In the first part of the present work we concentrate on aspect (ii) and therefore adopt a simple embedding scheme using a point charge array, which allows us to obtain information about methodological requirements and about the chemical reaction taking place. This, in turn, can then be transferred to larger, more realistic models of the reaction site, including relaxation effects, as is achieved in the second part of this study.

[†] The Royal Institution.
[‡] Imperial College.
[⊗] Abstract published in *Advance ACS Abstracts,* November 1, 1997.

S1089-5647(97)02198-6 CCC: $14.00

A major requirement resulting from objective (ii) is the need for a sufficiently high level of approximation underlying the electronic structure calculations. The reaction that is to be described involves the breaking and making of bonds, leading to the radical species $^{\bullet}CH_3$ (doublet). To represent this properly and with sufficient accuracy, quantum mechanical ab initio calculations are required. The unrestricted Hartree−Fock (UHF) approach is used as a starting point, but the nature of the process may make it necessary to go beyond this level. To improve the description, an adequate representation of electron correlation effects is needed. Starting from HF, this can be achieved by means of perturbation theory (e.g., MP2 or MP4). Alternatively, density functional theory (DFT) in one of its gradient-corrected implementations may be used. The latter has the advantage of being computationally less demanding, and therefore, application to large clusters (which is mandatory in the further course of this study; see below) is feasible. In particular, this study reports for the first time the application of a fully self-consistent DFT methodology to this problem. One previous study has included density functional correlation corrections[13] but applied a posteriori to the density calculated from the Hartree−Fock wave function. A comparison of the approaches has been performed using a small cluster model, and the results will be discussed in section 3.1.

Once the suitability of the methodology has been tested, requirement (i) must be reconsidered. Only a sufficiently large cluster model will allow an estimate of geometric relaxation effects throughout the course of the process studied. Therefore a much larger model is introduced in the second part of the study, resulting in an improved (i.e., more realistic) representation of the surface. In section 3.2 the consequences of employing such larger, nonrigid clusters are presented. Our results indicate significantly different geometries for the surface defect sites compared with those obtained previously, owing to the larger relaxations found in the present study.

The partitioning of the tasks as described above is needed, since otherwise the computational requirements would become immense. Undoubtedly an approach combining both a high level of theory and a good model cluster seems desirable. It seems, however, that since this is not feasible, the approach taken here still leads to a reliable determination of the energetics of the reaction studied.

2Computational Details

2.1. Minimal Cluster Model. For a model description of the interaction between methane and a $[Li]^0$ center, a site on the (100) surface of MgO has been chosen. For the electron hole to abstract efficiently a hydrogen atom from the approaching molecule, localization on a surface oxygen ion was assumed.[23] To stabilize this state, substitution of Mg^{2+} by Li^+ next to the oxygen ion is considered. There are two different possible positions for such a substitution, either in the first or in the second layer. To keep the model as simple as possible, Li has been placed in the second layer. This is the energetically preferred position found in a very recent slab calculation.[24]

Therefore, a minimal model (Figure 1a) of the site just described consists of one lithium and one oxygen ion (even Li could be represented by a PC, but in that case one would have to fix the position of oxygen). Such a model clearly has major limitations, since the oxygen wave function is not properly confined, and as shown by Pascual and Pettersson,[25] such models lead to errors in the local electrostatic potential. However, it has also been demonstrated by Børve and Pettersson[8] that there is only a small effect of the order of $\sim$ 1 kcal/mol on reaction

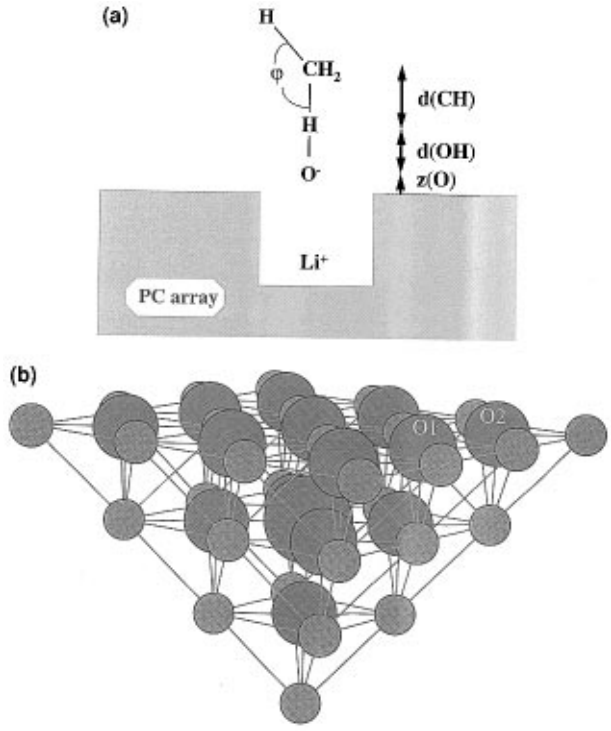

Figure 1. Cluster models of $[Li]^0$ center on MgO(100). Part a shows the minimal model $[MgO]Li^+O^-$ cluster interacting with CH_4. The oxidic crystal surface, [MgO], is represented by PCs. Upon variation of the distances d(CH) and d(OH) only φ and z(O) are optimized while lithium, replacing one of the magnesium ions, is not relaxed. Part b shows large cluster $Li^+O^-[Mg_{29}O_{13}]^{32-}$.

energetics arising from this inadequacy. Clearly, use of a much larger cluster is desirable. There are, however, also some drawbacks to the usefulness of large clusters in a study, such as the present one. Apart from the high computational expense, the following two disadvantages must be considered. (i) As the density of electronic states at the Fermi edge rises with cluster size, many low-lying states will hamper a straightforward SCF convergence to the ground state (in this case, smearing out the electron distribution across the Fermi edge can be useful to achieve convergence). (ii) The localization of the electron hole at the surface oxygen ion, guaranteed in the minimal model, may be hard to reproduce as more oxygen ions are treated explicitly; indeed, this proves extremely difficult without an adequate relaxation of at least the shell of nearest-neighbor atoms, which in turn implies the use of rather large clusters (see below).

Fortunately, the comparison of different levels of theory utilized in the quantum chemical description can be performed with a sufficient degree of accuracy using the minimal model $[MgO]Li^+O^-/CH_4$ (Figure 1a) as described above. This of course requires that the array of PCs used to embed the cluster model represents the effect of the surrounding lattice well. For the embedding of the minimal cluster model an array comprising almost 200 PCs in four crystal layers has been used ($4 \times 7 \times 7$). Comparison with calculations including some 750 PCs show that the results obtained with the present model of the Madelung field are well converged with respect to the size of the PC array. In all cases, full ionicity was assumed for magnesium oxide (i.e., $q = \pm 2.0$e). There has been some debate recently about the degree of ionicity of MgO.[16,17,26] This, however, seems to be a conceptual rather than a physical issue. For practical purposes, values of $q \neq \pm 2.0$e have not been found to yield more accurate results[27] and are therefore not considered here except for test purposes (see section 3.1).

2.2. Cluster Models. Even though the $[Li]^0$ center is charge neutral, it induces considerable geometric changes in the MgO lattice. Naturally, the ions adjacent to the defect site are affected most. To represent this relaxation in the cluster model, it is therefore necessary to optimize the positions of the shell of nearest-neighbor ions of lithium and of the central oxygen ion. This, of course, is not possible in the minimal cluster model introduced in section 2.1. At least one more shell of next nearest-neighbor ions, which are kept fixed with respect to the surrounding point charge array, must be included to terminate the cluster. Furthermore, to avoid artificial deformation of the charge distribution on the cluster (electron density spilling out into the charge array), no anions are allowed at cluster surface sites forming the interface between cluster and the point charge array. Following these considerations, a Li^+O^- $[Mg_{29}O_{13}]^{32-}$ cluster has been constructed (Figure 1b). We note that this cluster is larger than any used in previous studies, including the recent work of Johnson et al.[28] Under C_{4v} symmetry eleven degrees of freedom remain to be optimized. Owing to its size, this cluster requires embedding in a point charge array of about 750 charges. Owing to the expense of calculations on a cluster of this size, optimization has been restricted to a smaller subspace in some parts of the study (see section 3.2).

2.3. Electronic Structure Calculations. An adequate treatment of a reaction step in a catalytic process will involve inclusion of electronic degrees of freedom. Clearly, these must be described sufficiently well by the method chosen to determine the geometric and energetic properties of the system. Therefore, electronic structure calculations from first principles are required. The standard approach to this challenge comprises methods based on (a) Hartree−Fock (HF) theory and (b) density functional theory (DFT). Comparing them, one has to take into account the accuracy of the results obtained and the computational cost involved.

Simple HF calculations (UHF in the present case, since open shell reactants and products are involved) will always be useful in providing a point of reference, although the quantitative accuracy (e.g., for barrier heights or geometries) may be far from sufficient for a realistic treatment of the reaction. From a theoretical point of view, clearly the absence of electron correlation is a major deficiency. To amend for this shortcoming, perturbative treatment of correlation effects may be utilized. Møller−Plesset perturbation theory of second and fourth order (MP2 and MP4), although increasingly demanding in terms of computational cost and resources, has become a popular way to do this. In general, considerable improvement over simple HF may result in cases where the neglect of electron correlation introduces serious errors.

As an alternative to HF and post-HF schemes, DFT-based approaches lead to rather accurate results for ground-state minimum energy configurations at comparatively little computational effort. Here, in principle, electron correlation is included. Unfortunately, however, the appropriate form of the density functional (more specifically, its exchange correlation part, E_{xc}) is not known exactly. Therefore, in practical applications one is forced to use approximate functionals. One of the simplest ways is through the local density approximation (LDA), which has been widely used but is known to reproduce energetics only poorly. In recent years this problem has been largely overcome by the increasing use of nonlocal corrections. However, the accuracy of even gradient-corrected functionals for transition-state energies cannot be relied upon, and therefore, it is important to evaluate this aspect.

In this present work, HF, post-HF, and DFT calculations are employed to study the usefulness of DFT in application to the system studied. Although MP2 and MP4 can be treated for the very simple model used in section 3.1, an application to more realistic surface cluster models is computationally too demanding. DFT, on the other hand, scales more favorably and thus remains the method of choice to treat large cluster models without neglecting electron correlation. All calculations in section 3.1 have been performed using the CADPAC 6.0 code. Gradient corrections to the exchange and correlation functional have been used (B-LYP[29,30]).

Most calculations have been performed using a (8-411 G) Gaussian basis set for oxygen and 8-511G for Mg, where the exponents have been previously optimized for use in an ionic environment based on periodic Hartree−Fock calculations, and 6-31 G basis sets for H, Li, and C. For comparison, some calculations have been repeated with considerably larger basis sets (also including polarization functions). The effects observed are small, and they do not alter the conclusions drawn from the present study.

The results reported in section 3.2 have been obtained using the GAUSSIAN94 program. Since this code does not permit geometry optimization in the presence of point charges, the relaxation was carried out manually by iterative minimization with respect to each variable.

3. Results and Discussion

3.1. Comparing Different Levels of Theory. The reaction of methane with a $[Li]^0$ center,

$$CH_4 + [MgO]Li^+O^- \rightarrow {}^\bullet CH_3 + [MgO]Li^+(OH)^- \quad (3.1)$$

involves breaking of one of the CH bonds and formation of an OH bond. To allow both of these steps to occur simultaneously, a two-dimensional parameter subspace is considered by varying the distances d(CH) and d(OH) (as defined in Figure 1a) on a grid. For each pair of values (total of 100) the remaining parameters, φ and z(O) are allowed to relax. The total energy is then plotted as a contour plot in two dimensions. The results for HF, MP2, and BLYP calculations are shown in parts a, b, and d of Figure 2, respectively. For the MP4 calculation (Figure 2c) the values of φ and z(O) have not been optimized; instead, their optimized values from MP2 calculations have been used.

The HF and post-HF energy surfaces display the classical structure of an activated reaction: the reactants (R) are represented by the valley at the upper left, the transition state (TS) by a saddle point, and the products (P) by another valley at the lower right. This is the same topology as that from HF calculations on a rather simple model system (not including any representation of the Madelung field).[5] There, however, a late TS was found, whereas here the TS is rather symmetric (Figure 2a), which corresponds to the findings of a recent periodic calculation.[13] At the MP2 and MP4 level we even find an early TS (parts b and c of Figure 2).

The DFT calculations (Figure 2d) lead to a somewhat modified picture. No saddle point on the energy hypersurface is found for the hydrogen transfer from the methane molecule to the surface. There is, however, an energy barrier to be overcome as the resulting ${}^\bullet CH_3$ fragment leaves the surface.

To analyze the results obtained by different methods in more detail, calculations have been performed along an assumed reaction path, depicted by × in parts a−d of Figure 2. The corresponding energy profiles are shown in curves a−d of Figures 3, respectively. In each case the energy scale has been adjusted by subtraction of $E({}^\bullet CH_3) + E([MgO]Li^+(OH)^-)$, i.e., the sum of the energies of the products. In the HF calculations some 0.8 eV are required to reach the transition state as methane

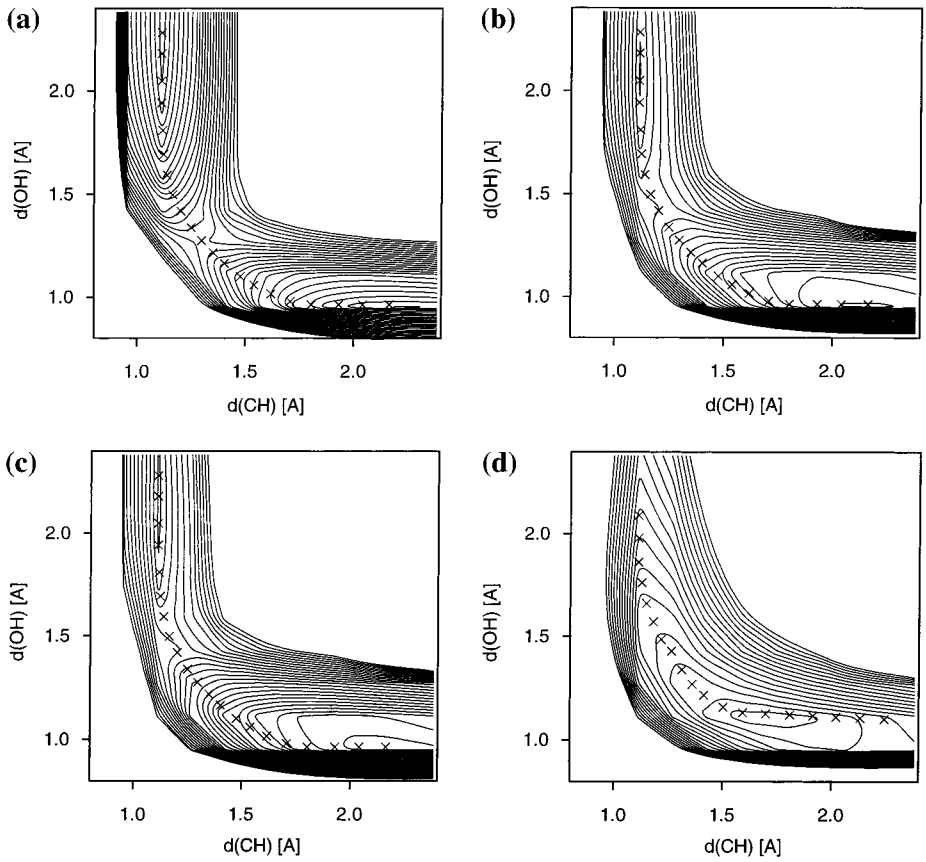

Figure 2. Energy surfaces of the system $[MgO]Li^+O^- - CH_4$ as calculated using (a) HF, (b) MP2, (c) MP4, and (d) DFT:B-LYP. In each case, the bond distances of the CH and OH bond have been varied, while the remaining variables (see Figure 1) have been allowed to relax. Contour lines are drawn at 54 meV differences. The path denoted × was used in the calculations represented by Figure 3.

TABLE 1: Geometrical Parameters (in Å) and Energies (in eV) Characterizing the Reaction of $[MgO]Li^+O^-$ with CH_4 As Computed by Various Methods Where ΔE_A is the Activation Energy and ΔE_R is the Reaction Energy[a]

system	parameter[b]	HF	MP2	MP4	DFT[c]	DFT[d]
	ΔE_A/eV	0.83	0.08	0.05		
	ΔE_R/eV	0.15	−0.57	−0.41	−0.35	
	d(OH)/Å	1.28	1.45	1.45	1.43	1.13
	d(CH)/Å	1.30	1.25	1.22	1.26	1.70
$[MgO]Li^+O^-/CH_4$	*φ*/(deg)	104	107	(107)[e]	104	98
	z(O)/Å	0.30	0.24	(0.24)[e]	0.28	0.34
CH_4	*d*(CH)/Å	1.08	1.10	1.10	1.10	
Li^+OH^-	*d*(OH)/Å	0.97	1.00	1.00	1.00	
	z(O)/Å	0.40	0.40	0.40	0.39	
Li^+O^-	*z*(O)/Å	0.18	0.18	0.18	0.18	

[a] For comparison the DFT results at the shoulder of the energy profile (see text and Figure 2d) have been included. The data reported for CH_4 refer to the isolated molecule, those for Li^+OH^- to the product species on the surface; and those for LiO^- to the initial surface $[Li]^0$ species. [b] See Figure 1. [c] Values of the geometrical parameters at the shoulder. [d] Values of the geometrical parameters at the minimum. [e] From MP2 calculation.

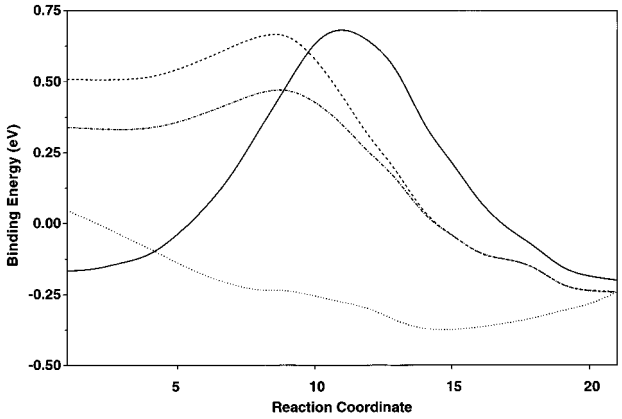

Figure 3. Energy profile (in eV) along the reaction path shown in Figure 2: (a) HF (solid); (b) MP2 (dashed); (c) MP4 (dash−dotted); (d) DFT:B-LYP (dotted). In each case the zero of energy scale has been set to the sum of the energies of the products.

approaches the oxygen ion. This happens at a CH bond length elongated by more than 0.2 Å with respect to the equilibrium distance in methane (1.08 Å), while *d*(OH) assumes a value of about 0.3 Å above the equilibrium length calculated for the product species $[MgO]Li^+(OH)^-$. This onset of OH bond formation is partially due to a movement of the oxygen ion further away from the surface, as is apparent from the values of *z*(O) reported in Table 1.

On inclusion of the MP2 (and MP4) energy corrections, the maximum in the profile corresponding to the transition state is shifted to an earlier point along the reaction coordinate (curves b and c of Figure 3). The activation energy to reach this point amounts to less than 10% of the value found from HF calculations (see Table 1). Here, the elongation of the CH bond is only 0.15 Å (even less for MP4), while conversely, the value of the OH bond length now lies 0.45 Å above its final value, i.e., the one adopted in the product system $[MgO]Li^+(OH^-)$. At the same time the distance between the oxygen ion and the first crystal plane is increased at the TS by only half the amount found without MP corrections. All these observations support the picture of an early TS.

When a similar reaction path in the DFT approach is followed (the coordinates of the points chosen to generate this path have been slightly modified, taking into account the somewhat different topology of the energy surfaces, as shown in parts a and d of Figure 2), the energy profile shown in Figure 3d is

TABLE 2: Activation Energy (eV) for the Reaction $H_2 + H^\bullet \rightarrow H^\bullet + H_2$ at Various Levels of Theory

method	energy
expt	0.421
BLYP/6-31G**	0.113
BLYP/6-311++G**	0.126
B3LYP/6-311++G**	0.184
HF-LYP/6-31G**	0.412
HF-LYP/6-311++G**	0.401
G2	0.450

obtained. In this case, no maximum (indicative of a TS) is seen, but the curve merely displays a shoulder at the position of the maximum in the MP2 and MP4 curves. The geometrical parameters characterizing this point are very close to those of the MP2 (and MP4) TS (see Table 1).

For large CH and large OH distances alike, the DFT description somewhat surprisingly shows a behavior different from that expected from the MP2 (and MP4) calculations. The behavior of the DFT solution is not due to the particular choice of basis functions or the PC array, as has been shown in various test calculations. The trend observed here is similar to the one found in a recent comparison of B-LYP DFT and CCSD(T) calculations on the reaction $H_2 + {}^\bullet H \rightarrow {}^\bullet H + H_2$, for which a TS at a rather low energy (with respect to the reactants and the products) has been found in the B-LYP scheme. In the present case, however, the magnitude of the effect is somewhat larger.[31] Assuming both observations to be due to a common cause, the correction of the (incorrect) self-interaction (SIC) in DFT should lead to an improvement of the resulting energy profile.[31] Unfortunately, the automatic inclusion of SIC is not readily available in most implementations of density functional theory.

Based on the prototypical system $H_2 + H^\bullet$, we have investigated how else the prediction of activation energies for hydrogen atom transfers may be improved. In the earlier study of Johnson et al.,[31] they compared the results of a wide range of pure density functionals, with and without SIC, against accurate quantum mechanical methods and experiment. We have extended these results to include hybrid functionals (Table 2) using a 6-311++G** basis set.

From these results, we can clearly see the severe underestimation of the activation energy by the BLYP functional without SIC. Even the widely used hybrid functional B3LYP is considerably in error. However, if Hartree−Fock exchange is used and only the LYP correlation functional is retained, then good agreement with experimental results is found. Similar results are obtained with other nonlocal correlation functionals. Hence, these preliminary results suggest that it may be possible to obtain accurate results from DFT calculations for this type of reaction by use of Hartree−Fock exchange with a correlation functional without recourse to the use of self-interaction correction.

3.2. Importance of Cluster Model Size and Substrate Relaxation. The model used in section 3.1, though very useful for the comparison of different levels of theory in the electronic structure calculation, is far from being a realistic representation of the surface site or its interaction with the methane molecule. It suffers from the geometric approximation of a bulk-terminated surface and from the fact that, through the point charges, only the electrostatic influence of the surrounding is modeled while Pauli repulsion and substrate polarization are absent. To refine the model, it is therefore necessary to include more atoms in the cluster (treated quantum mechanically) and to allow partial relaxation. These considerations lead to the construction of a larger cluster model (see section 2.1 and Figure 1b). For reasons of computational economy, calculations involving this cluster are limited to the HF level.

TABLE 3: Atomic Relaxations (in Å) of the XY $[Mg_{29}O_{13}]^{32-}$ Clusters Representing (a) Clean MgO (100) Surface ($XY = Mg^{2+}O^{2-}$), (b) a $[Li]^0$ Center on MgO (100) ($XY = Li^+O^-$), and (c) Hydroxylated $[Li]^0$ Center ($XY = Li^+(OH)^-$)[a]

layer	atom(s)[c]	coordinate	$Mg^{2+}O^{2-}$	Li^+O^-	$Li^+(OH)^-$
first	O^-/O^{2-}	z	0.00	0.28	0.35[b]
	Mg	x/y	0.03	0.12	0.11
		z	−0.03	−0.07	−0.10
	O1	$x = y$	0.02	0.01	0.00
		z	0.00	0.01	0.01
second	Li^+/Mg^{2+}	z	−0.05	−0.29	−0.27
	O	x/y	0.02	0.08	0.09
		z	−0.02	0.02	0.01
third	O	z	−0.03	−0.10	−0.10

[a] The values given are the deviations from the ideal (bulk termination) structure. [b] Equilibrium value of the OH distance is 0.96 Å. [c] For labeling of oxygens, see Figure 1. O are the unlabeled oxygens in the figure.

Before this cluster is employed in the study of the reaction of methane with the defect center, three surface structures are investigated: pure MgO, the $[Li]^0$ center and the $Li^+(OH)^-$ surface species that is formed in reaction 3.1. For each case, the relaxed geometry obtained at the HF level is given in Table 3.

For the cluster representing a perfect MgO surface, geometry optimization leads to small deviations from the idealized, bulk-terminated structure with differences of $<0.005-0.05$ Å. This is in excellent agreement with the experimental finding of little (less than 3%) surface relaxation on MgO(100),[32,33] which is also supported by other theoretical work.[28,34,35]

Introducing a $[Li]^0$ defect, on the other hand, has a considerable effect on the geometry of the cluster. This relaxation effect is caused by the lower charge of O^- and Li^+ compared to O^{2-} and Mg^{2+}, respectively. Although the defect is overall charge neutral, its electrostatic interaction with surrounding ions is reduced. These in turn show a tendency to move away from the defect site, which is reflected in the geometric changes of ions directly adjacent to the $[Li]^0$ center. Even more affected, however, are the ions of the $[Li]^0$ center itself, moving by approximately 10% of the bulk Mg−O distance. The relaxation energy (calculated as the difference of the cluster energies corresponding to the optimized and the unrelaxed structure) amounts to 1.9 eV.

The third model listed in Table 3 represents one of the products of reaction 3.1, a $Li^+(OH)^-$ species. On comparison of its geometry to the $[Li]^0$ center an even stronger relaxation is observed. Apart from the position of the central oxygen atom (on which formally the hole is localized), however, the differences do not exceed 0.03 Å. This observation suggests that the additional hydrogen atom causes no drastic change in the electrostatic force balance governing the calculated cluster geometry. The validity of this conclusion is strongly supported by an analysis of Mulliken charges. In Table 4 they are listed for the two clusters. Again, the largest change takes place at the central anion, but even there it amounts to only 0.03e (if one adds up the electron population of hydrogen and oxygen in the $(OH)^-$ species). For the $Li^+(OH)^-$ cluster a relaxation energy of 2.7 eV was calculated.

It is instructive to compare our calculated relaxed geometries with those reported by Orlando et al.[13] based on periodic HF techniques. For the $[Li]^0$ center we obtain a displacement for the O^- of 0.28 Å compared with 0.32 Å in the latter study. Our calculations include relaxation of the second shell of ions, unlike the study of Orlando et al.; the more restricted relaxation in the latter leads to a larger displacement of the O^- out of the surface plane. The effect is even more pronounced in the case of the surface OH, where Orlando et al. calculate a displacement of

TABLE 4: Mulliken Charges of the XY $[Mg_{29}O_{13}]^{32-}$ Clusters Representing (a) Clean MgO (100) Surface (XY = Mg^{2+} O^{2-}), (b) $[Li]^0$ Center on MgO (100) (XY = Li^+O^-), and (c) Hydroxylated $[Li]^0$ Center (XY = $Li^+(OH)^-$)[a]

layer	atom(s)	$Mg^{2+}O^{2-}$	Li^+O^-	$Li^+(OH)^-$
first	O^-/O^{2-}	−1.97	−1.03	−1.06
	Mg	1.89	1.86	1.87
	O1	−1.89	−1.88	−1.88
	O2	−1.91	−1.91	−1.91
second	Li^+/Mg^{2+}	1.92	0.89	0.91
	O	−1.97	−1.92	−1.93
third	O	−1.98	−1.93	−1.94

[a] The values given are taken from HF calculations at the relaxed geometry (see Table 2). To the magnesium atoms on the border of the cluster, Mulliken charges of 1.96−1.99 are assigned.

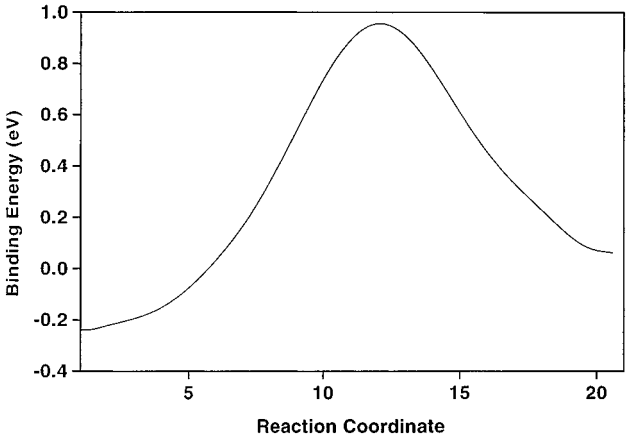

Figure 4. Energy profile (in eV) as in Figures 3a using a larger cluster model (see text) with HF techniques.

0.58 Å compared with our value of 0.35 Å. We also note that the more restricted relaxation employed in ref 13 also reduces the Mg displacement by up to 50% compared with those obtained in our calculations. It is interesting to observe that the recent cluster calculations in ref 28 used a more restricted relaxation than that employed by Orlando et al. and found even larger OH displacements. These results underline the importance of using extensive relaxation if accurate geometries are to be obtained.

These results guide the route taken in the last part of this study because they allow us to make a simplifying assumption in the treatment of cluster relaxation throughout reaction 3.1. To study the effect of surface relaxation on the energy profile along a reaction path (the same path as in section 3.1 is used), it is desirable to reduce the number of degrees of freedom in these calculations. Therefore, only one substrate mode is studied: the one defined by the two geometries of the free and the hydroxylated $[Li]^0$ center. In particular, the mean geometry between those two was chosen as a reference point. For selected points along the reaction path the energy calculated at this geometry was found to be 0.01−0.07 eV higher than the minimum energy (minimizing with respect to this one degree of freedom only), the largest differences occurring toward the end of the reaction. We can thus estimate the error introduced as the substrate is frozen at the intermediate geometry.

The full energy profile of reaction 3.1 along the path shown in Figure 2a was calculated at the HF level using the values of φ obtained from the minimal cluster study (section 3.1). The curve obtained is shown in Figure 4. The general shape and the position of the maximum are the same as for the minimal cluster study (Figure 3a). The activation barrier, however, is higher by 50% at about 1.2 eV. The result is, however, close to that obtained in the earlier cluster calculations in ref 8 for which a value of 1.13 eV is reported and that obtained using periodic boundary techniques[13] where the same value of 1.13 eV was also calculated. The calculations in ref 28 did not report activation energies. It appears, however, that calculated activation energies are relatively insensitive to cluster size, provided a first shell of neighbors is included. The barrier height is, however, very sensitive to the correlation treatment, which greatly reduces its magnitude. We note that when we repeated our calculation using DFT methods, based on the BLYP functional, we again found very low activation energies as in the smaller cluster studies. In contrast, Orlando et al. found a potential energy surface with a reasonable activation energy of 0.78 eV, when including only correlation a posteriori. This further confirms that the use of the density functional exchange potential is responsible for the anomalously low activation energies obtained using most DFT methods.

We also note that the reaction is now calculated to be endothermic, in this case with an energy difference of some 0.25 eV. The difference between this value and that obtained for the smaller cluster is not surprising. The larger model not only incorporates the substrate relaxation but also gives a much better description of polarization effects in the vicinity of the reaction site. The calculated reaction energy compares with the value of 0.39 eV obtained by Børve and Pettersson[8] and −0.001 eV reported by Orlando et al.[13] Inclusion of relaxation favors the products, since, as noted earlier, the hydroxyl group relaxes more extensively than the O^-. The use of the larger cluster in our calculation compared with that in ref 8 therefore reduces the calculated endothermicity, which disappears in the results obtained in ref 13 owing to the very large OH displacement obtained in that study.

4. Conclusions

Theoretical modeling of the interaction between methane and a defect at the surface of MgO leading to a CH bond breaking requires the utilization of electronic structure methods of a high theoretical level. Applying HF, post-HF schemes, and DFT to a simple model of the system, it becomes obvious that an adequate description of the energetics of this process can only be given when electron correlation is, in some way, included in the electronic structure calculation. To do this in a systematic but unfortunately rather expensive way, one may use MP2 or MP4 methods. For the reaction studied here a substantial lowering of the activation barrier (compared to HF) is observed. Alternatively, the computationally much less demanding DFT, including gradient corrections, leads to an even stronger change in the energy profile. Here, only a shoulder remains of the energy barrier, and the reaction proceeds without an activation energy. This spurious effect can be attributed to the self-interaction correction error in the exchange energy. On comparison of the overall reaction energy, DFT and MP4 yield similar results.

In a complementary study (restricted to the HF level), an improved cluster model was used. This in itself leads to a much better description of the geometric structure of the $[Li]^0$ center. The much more extensive relaxation employed in the present cluster calculations compared with that reported previously has a substantial effect on the calculated geometries. In particular, the relaxed surface structure becomes relatively insensitive to the nature of the defect (O^- or OH), which is not apparent in the previous studies, when relaxation is only included in the first shell. The effect on the activation energies of these relaxation effects are, however, relatively small. And in our model, where relaxation effects are similar in reactants and products, it may be a reasonable approximation to include

relaxation effects in a static way, assuming a substrate geometry by averaging the geometries found for the reactant and product cluster.

Acknowledgment. We are grateful to EPSRC for provision of a ROPA grant supporting this work. We are grateful to Prof. Sir John Meurig Thomas for many useful discussions relating to this work.

References and Notes

(1) Hutchings, G. J.; Scurrell, M. S.; Woodhouse, J. R. *Chem. Soc. Rev*. **1989**, *18*, 251−283.
(2) Lunsford, J. H. *Angew. Chem., Int. Ed. Engl*. **1995**, *34*, 970−980.
(3) Pope, S. A.; Guest, M. F.; Hillier, I. H.; Colbourn, E. A.; Macrodt, W. C.; Kendrick, J. *Phys. Rev.* **1983**, *B28*, 2191−2199.
(4) Mehandru, S. P.; Anderson, A. B.; Brazdil, J. F. *J. Am. Chem. Soc*. **1988**, *110*, 1715−1719.
(5) Zicovich-Wilson, C. M.; Gonzalez-Luque, R.; Viruella-Martin, P. M. J. *Mol. Struct.: THEOCHEM* **1990**, *208*, 153−162.
(6) Viruella-Martin, P. M.; Viruella-Martin, R.; Zicovich-Wilson, C. M.; Tomas-Vert, F. *J. Mol. Catal*. **1991**, *64*, 191−200.
(7) Børve, K. J.; Pettersson, L. G. M. *J. Phys. Chem*. **1991**, *95*, 3214−3217.
(8) Børve, K. J.; Pettersson, L. G. M. *J. Phys. Chem*. **1991**, *95*, 7401−7405.
(9) Børve, K. J. *J. Chem. Phys*. **1991**, *95*, 4626−4631.
(10) Anchell, L. J.; Morokuma, K.; Hess, A. C. *J. Chem. Phys*. **1991**, *99*, 6004−6013.
(11) Kobayashi, H.; Salahub, D. R.; Ito, T. *J. Phys. Chem*. **1994**, *98*, 5487−5492.
(12) Zhidomirov, G. M.; Avdeev, V. I.; Zakhardov, I. I.; Zhanpeisov, N. U.; Yudanov, I. V. *Catal. Today* **1995**, *24*, 383−387.
(13) Orlando, R.; Cora, F.; Millini, R.; Perego, G.; Dovesi, R. *J. Chem. Phys*. 1996, 105, 8437.
(14) Driscoll, D. J.; Martir, W.; Wang, J. X.; Lunsford, J. H. *J. Am. Chem. Soc*. **1985**, *107*, 58.
(15) Lopez, T.; Gomez, R.; Ramirez-Solis, A.; Poulain, E.; Novaro, O. *J. Mol. Catal*. **1994**, *88*, 71−84.
(16) Neyman, K. M.; Rösch, N. *Chem. Phys*. **1992**, *168*, 267−280.
(17) Pacchioni, G.; Neyman, K. M.; Rösch, N. J. Electron. *Spectrosc. Relat. Phenom*. **1994**, *69*, 13−21.
(18) Ferrari, A. M.; Pacchioni, G. *J. Phys. Chem*. **1995**, *99*, 17010−17018.
(19) Pacchioni, G.; Ferrari, A. M.; Giamello, E. *Chem. Phys. Lett*. **1996**, *255*, 58−64.
(20) Vail, J. M. *J. Phys. Chem. Solids* **1990**, *51*, 589−607.
(21) Grimes, R. W.; Catlow, C. R. A.; Shluger, A. L.; Baetzold, R.; Pandey, R. *Ceram. Trans.* **1991**, *24*, 269−275.
(22) Shluger, A. L. *Phys. Rev.* **1996**, *B54*, 562.
(23) Shluger, A. L.; Heifets, E. N.; Gale, J. D.; Catlow, C. R. A. *J. Phys.: Condens. Matter* **1992**, *26*, 5711−5722.
(24) Birkenheuer, U.; Cora, F.; Pisani, C.; Scorza, E.; Perego, G. *Surf. Sci*. **1997**, *373*, 393−408.
(25) Pascual, J. L.; Pettersson, L. G. M. *Chem. Phys. Lett*. **1997**, *270*, 351−6.
(26) Rösch, N.; Neyman, K. M.; Birkenheuer, U. Density functional investigations of adsorption at metal oxide surfaces. In *Adsorption on Ordered Surfaces of Ionic Solids and Thin Films*, Freund, H.-J., Umbach, E., Eds.; Springer Series in Surface Sciences 33; Springer-Verlag: Berlin, 1993; pp 206−218.
(27) Neyman, K. M.; Rösch, N. *Surf. Sci*. **1993**, *297*, 223−234.
(28) Johnson, M. A.; Stefanovich, E. V.; Truong, T. N. *J. Phys. Chem. B* **1997**, *101*, 3196−3201.
(29) Becke, A. D. *Phys. Rev*. **1988**, *A38*, 3098.
(30) Lee, C.; Yang, W.; Parr, R. G. *Phys. Rev*. **1988**, *B37*, 785−789.
(31) Johnson, B. G.; Gonzales, C. A.; Gill, P. M. W.; Pople, J. A. *Chem. Phys. Lett*. **1994**, *221*, 100−108.
(32) Welton-Cook, M. R.; Berndt, W. *J. Phys*. **1982**, *C15*, 5691.
(33) Urano, T.; Kanaja, T.; Kaburagi, M. *Surf. Sci*. **1983**, *134*, 109.
(34) Colbourn, E. A.; Mackrodt, W. C. *Solid State Ionics* **1983**, *8*, 221.
(35) Causa, M.; Dovesi, R.; Pisani, C.; Roetti, C. *Surf. Sci*. **1986**, *175*, 551.